Pyrite Sensitized ZnO-Nanorods and ZnO-Nanoparticles based Solar Cells: Photoelectrochemistry and Mechanistic comparative Studies

Idriss Bedja

Cornea Research Chair, Department of Optometry, College of Applied Medical Sciences, King Saud University, Saudi Arabia

Abstract: Thin films of ZnO semiconductor nanorods (ZnO-nr) of 6 um length have been sensitized with FeS_2 ultra fine particles. Both the optical absorption and the photocurrent action spectra of ZnO-nr, ZnO nanoparticulate (ZnO-np) electrodes were extended to visible region, upon coating with FeS_2 particles, by sensitization mechanism. Quantum size effect is manifested by a blue shift in both absorption and photocurrent action spectrum. PIA (Photoinduced absorption spectroscopy), where the excitation is provided by a square-wave modulated (on/off) monochromatic diode light source, is a multipurpose tool in the study of dye-sensitized solar cells. Here, we use PIA as a tool for the study of a quantum-dot modified metal oxide nanostructrued electrode. The PIA spectra showed an evidence for long-lived photoinduced charge separation. Time-resolved PIA showed that recombination between electrons and holes occurs on a millisecond timescale. Incident-Photon-to-Current Efficiency about 25% has been obtained at 400 nm excitation for ZnO-nr electrodes comparing only 13% for ZnO-np electrodes. ZnO-nr (1D network) based pyrite photoelectrode shows best photoresponse and e-transfer mechanistic than ZnO-np based pyrite solar cell. The better solar cell performance of FeS_2 on ZnO-nr over ZnO-np can be ascribed to the faster, unidirectional e-transport channels through the ZnO-nr as well as the longer electron lifetimes. The lower performances of electrodes can be explained by the presence of FeS_2 phases other than the photoactive pyrite phase, as evidenced from XRD study

KEYWORDS - FeS_2, Quantum-dots, ZnO-n anorods, PIA, Photoelectrochemistry

I. INTRODUCTION

A great effort is being done to obtain efficient and inexpensive organic and inorganic solar cells. The approach of using semiconductor colloids for the design of optically transparent thin semiconductor films is considered as the unique and the alternative for the amorphous silicon solar cells. Under this approach, Nanostructured solar cells sensitized by organic dyes (DSSC) [1-4] or by inorganic short band gap semiconductors (also called quantum dots, QDs) [5-8] have attracted a great deal of interest because of their efficient conversion of solar energy to electricity at a low cost compared to conventional semiconductor photovoltaic devices. This is primarily because they are quite stable and because they predominantly absorb in the UV. The usefulness of these systems for solar cell applications was made possible by a basic principle namely, sensitization of their semiconductor surfaces into visible region either by organic dyes or by inorganic short band gap semiconductors also called quantum dots (QDs) (semiconductor sensitization). Power conversion efficiencies in the range of 8-12% in diffuse daylight have been obtained in the sensitization of highly porous TiO_2 film with only a submonolayer required ruthenium complex.[1] In the other hand, wide band gap semiconductors have been sensitized by short band gap (quantum dots) semiconductor materials ($CdSe/TiO_2$[4], CdS/TiO_2-SnO_2[8]) as alternative to dye sensitization. Vogel and co-workers [6] have investigated the sensitization of nanoporous TiO_2, ZnO by Q-sized CdS, Photocurrent quantum yields of up to nearly 80% and open circuit voltages up to 1 V range were obtained. In contrast with the dye sensitized solar cells, fundamental understanding of factors controlling the interfacial electron transfer reactions in Q-dots modified metal oxide based solar cells is limited. Photoinduced absorption spectroscopy (PIA) is a suitable and a lower costly (in contrast with laser spectroscopy) method to obtain spectral and kinetic information of the Q-dot sensitized MO electrodes. DSSC's (dye sensitized solar cells) based on one dimensional (1-D) ZnO nanostructures, which exhibit significantly higher electron mobility than that of both TiO2 and ZnO nanoparticulate (np) films [19], have recently been attracting increasing attention [19,21].

Here, instead of organic dye as in DSSC cells, we use FeS_2 quantum dots semiconductor to sensitize ZnO nanorods based films. FeS_2 (Pyrite) is another favorable candidate photosensitization material because of its environmental compatibility, high stability toward photocorrosion as well as very good absorption in the visible region of the solar spectrum. The pyrite polymorph of iron disulfide is of particular interest, and shows promise for solar energy conversion devices in both photoeletcrochemical and photovoltaic solar cells [9,10] and solid state solar

cells [11] due to its favorable solid state properties [12]. Ennaoui et al. have reported [12] interesting photoresponse of modified polycrystalline TiO_2 electrode with FeS2 using CVD method. Jing H. Fang et al. have first [13] reported a method of modification of TiO_2 large band gap (Degussa P25) by quantum sized FeS_2 particles by a similar procedure described originally by Chatzitheodorou [14]. They have reported an Incident-photon-to current efficiency of 25% at 400 nm excitation.

In this work, we report a modification of ZnO nanorod based films by quantum dots FeS_2 by a similar method described previously by Chatzitheodorou [14] on TiO2 films. Our results will describe photoelectrochemical properties and photoinduced absorption spectroscopy of ZnO modified FeS_2 quantum dots in comparison with ZnO nanostruc-tured based films.

II.   MATERIALS AND METHODS

2.1 Preparation of ZnO Nanorod (1D) Films
Firstly, 300 nm ZnO seed layer was prepared on the optically conducting glass, indium doped SnO2 (ITO) substrate. Two drops of 5 mM solution of zinc acetate dihydrtae in ethanol absolute, rinsed in ethanol and blown dry with nitrogen gas. This is repeated four times before sintering at 350 C in air for 30 min and cooled dow to room temperature. This process is repeated twice.

Secondly, the deposited ZnO seed substrate was immersed into an aqueous solution of 25 mM zinc nitrate hexahydrate; 25 mM hexamethylenetetramine and 5 mM polytheleneimine at 90 C for a hydrothermal reaction total 12 hours. The solution was replaced by a fresh one every 4 hours. The obtained ZnO nanorods were rinsed with deionized water and dried in air at room temperature.

2.2 Preparation of ZnO nanostructured Films
The concentration of ZnO colloids was 0.05 M and was prepared by the method described by Spanhel and Anderson with little change. Addition of LiOH to the organomettalic zinc complex solution was less by 25% than the required for stochiometric addition. Colloidal ZnO solution thus obtained does not need any further concentration since small amount of solvent was used. The diameter of these colloidal particles were in the range of 20-50 A. A small aliquot (0.1-0.8 ml) of ZnO sol was applied to a conducting surface (OTE: $0.8x4$ cm^2). The films (0.5 - 3 mm) are dried in air and then sintered at 673 K for 1 h. The semiconductor films sintered adhered strongly to the glass surface and were stable in neutral and alkaline solutions.

2.3 Surface Modification of ZnO by Quantum Dots F2S$_2$
ZnO metal oxide nanostructured and nanorod films are modified by quantum dots FeS2 by a similar method described previously by Chatzitheodorou [14] with little modification. The clean SnO2 electrode was dipped in the solution of sulfur (0.02 M) in xylene, followed by immersion in a solution of iron pentacarbonyl (0.01M) in xylene at the temperature close to 139 C. The whole experiment was carried out under a nitrogen atmosphere. This procedure was repeated several times until a clear dark color appears. The new in this procedure is the heating of the electrodes at 125 C for about 5 min after washing with xylene solvent between two immersions.

2.4 Characterization Method
UV-vis spectra were recorded using a Hewlett-Packard 8453 diode array spectrometer. The photoelectrochemical measurements were carried out in a layer quartz cell similar to that in Fig. 1 [also in Ref.22]. Two electrodes were inserted consisting of a reference (Ag/AgCl) and counter (Pt wire) electrodes. A Princeton Applied Research (PAR) Model 173 and 175 universal potentiostats were used in electrochemical measurements. The setups for recording incident photon to current efficiency (IPCE) spectra and I-V curves have been described elsewhere (see ref 15).
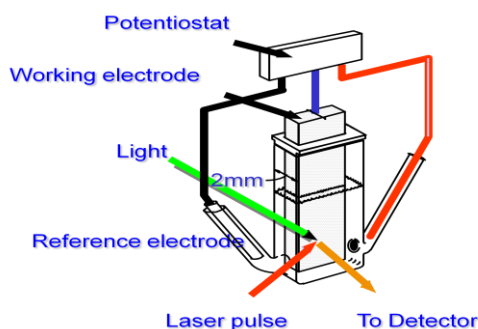

Fig. 1: Photoelectrochemical Cell (Quartz) [Bedja, Ph.D. Dissertation 1996]

For PIA spectroscopy (Fig. 2), excitation of the sample was provided by light from a blue LED (Luxeon Star 1W, Royal Blue, 470 nm), which was square-wave modulated (on/off) by electronical means using an HP 33120A waveform generator and a home- built LED driver system. The beam, with an intensity in the range of 0.5–30 mW/cm2, excited a sample area of about 1 cm2. White probe light was provided by a 20 W tungsten-halogen lamp. A cutoff filter (Schott RG715) was used to minimize excitation of the sample by the probe light where indicated. The transmitted probe light was focused
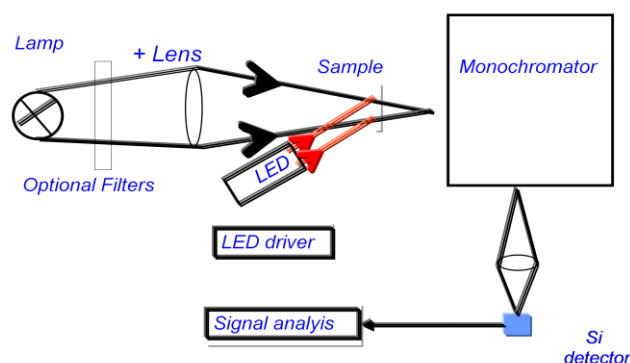

Fig. 2: Photoinduced Absorption Spectroscopy Set-up

onto a monochromator (Acton Research Corporation SP-150) and detected using a UV- enhanced Si photo-diode, connected to a lock-in amplifier via a current amplifier (Stan-ford Research Systems models 830 and 570, respectively). For the time-resolved studies the output of the current amplifier was connected to a data acquisition board (National Instruments PCI-6052E). All PIA measurements were done at room temperature.

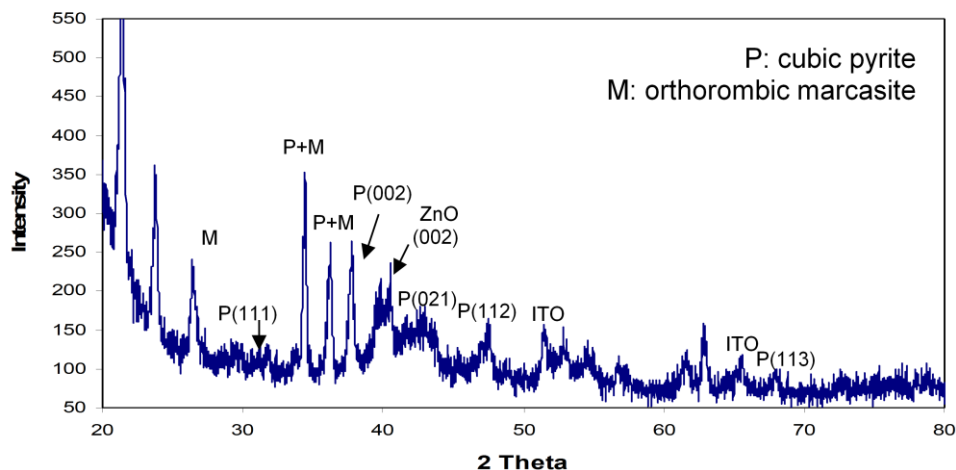## III.   RESULTS AND DISCUSSION

3.1 XRD and SEM

Fig. 3:   XRD spectrum of ZnO-nr particulate film after FeS_2 deposition

The X-ray diffraction (XRD) in Fig. 3 shows the (002) direction of the ZnO nanorods. FeS2 picks also appear to have multiple phases namely cubic (pyrite) and orthorhombic marcasite.   SEM image in Fig. 4 demonstrates a 1 dimensional network of ZnO nanorods about 6 μm length. The diameter of these nanorods was estimated to be less than 300 nm**.**
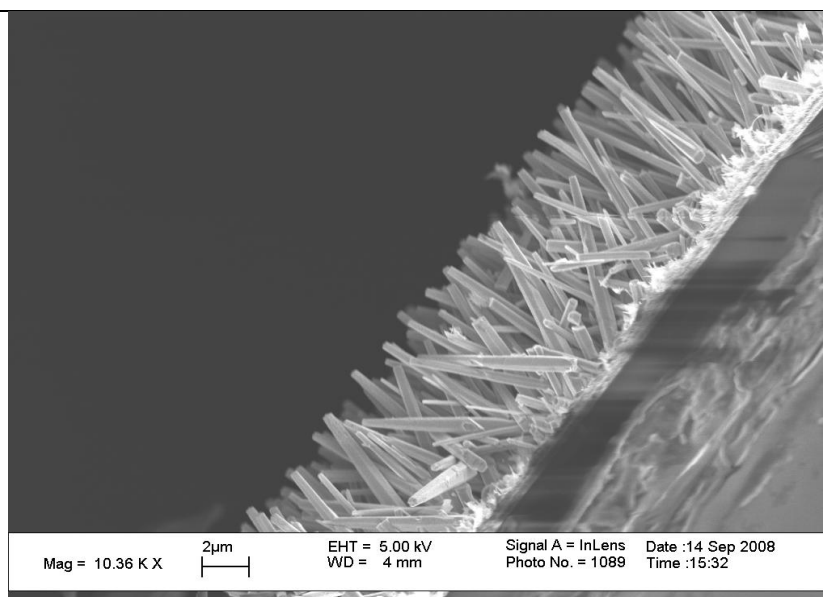
Fig. 4: SEM cross section picture of ZnO nanorods film. Inset is an SEM FeS2 filled ZnO nanorods film Inset image shows a large FeS2 adsorption around ZnO nanorods. FeS$_2$ quantum filled ZnO nanorods seem to aggregate to form large FeS$_2$ particles. This is also demonstrated by absorption spectra in Fig. 5.

3.2 Absorption and IPCE Spectra

Fig. 5A (a) shows the absorption spectrum of ZnO-nr film alone while Fig. 5 A(b) and depicts the absorption spectrum of FeS$_2$ modified ZnO-nr film showing a short wavelength absorption onset, although FeS$_2$ bandgap is small around 1 eV. We would expect a large wavelength absorption onset near IR. This might be explained either in term of non-stochiometric pyrite present in the film or a quantum size effect of very small
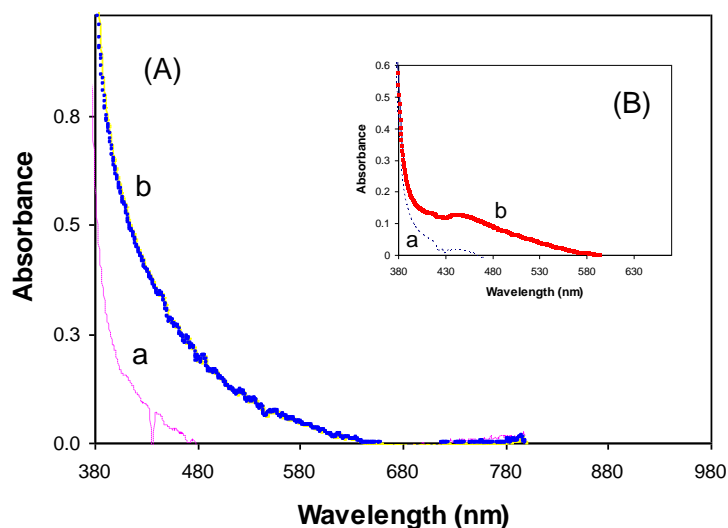

Fig. 5: Absorption spectra of A (a) ZnO nanorod alone and (b) ZnO nanorod film modified with successive layers of FeS2 particles. B (a) ZnO nanoparticulate film alone and (b) modified with FeS2 particles.

FeS$_2$ particles which causes a bandgap energy rising.   This significant blue shift of the absorption of ultra fine FeS$_2$ particles compared to a bulk crystalline [17] is also observed in colloidal FeS$_2$ particles in solution [18]. The low energy tail comes from large particles, while the high energy absorption shoulder of FeS2/ZnO electrode comes predominately from small particles. Although, ZnO nanoctructured are known to have large porosity compared to 1D ZnO network, here both ZnO-NP and ZnO-nr films (with almost similar thicknesses around 6 μm), seem to adsorb almost similar amount of FeS$_2$ Q-dot particles.

The photoelectrochemical response of the ZnO-nr electrode, before and after modification with FeS$_2$, was evaluated by measuring the photocurrent of the electrode at various excitation wavelengths. The incident photon-to-

photocurrent efficiency (IPCE) was then determined from the expression (1) where I_{sc} is the short-circuit current (A/cm^2), I_{inc} is the incident light intensity (W/cm^2), and λ is the excitation wavelength (nanometers).

$$IPCE\ (\%) = 100 \times (1240 \times I_{sc})/(I_{inc}\lambda) \qquad (1)$$

Fig. 6 depicts the photocurrent action spectra of ZnO electrodes (nr and np) before and after modification with FeS_2 particles. The photoresponse of ZnO-nr electrode (Fig. 6 A (a)) has been extended to the visible range after FeS_2 modification (Fig. 6 A (b)). In addition, we can see the blue shift of the absorption spectrum of FeS_2/ZnO-nr compared to a bulk FeS_2. This shift is understood in terms of the quantum size effect. Although the FeS_2 /ZnO electrode shows a visible absorption, spectrum in wavelengths longer than 580 nm, no photoresponse was detected at these wavelengths which suggest that only small quantum-sized FeS_2 particles play a dominant role in the spectral sensitization on ZnO-nr particles, while larger particles have less or no contribution. In the other side, ZnO-np photoectrodes show less photoresponse to visible spectrum than in ZnO-nr.
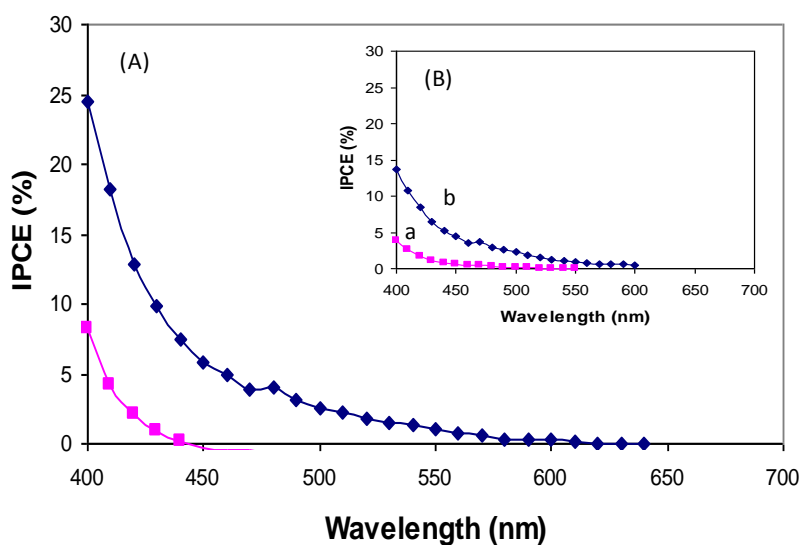

Fig. 6: Incident photon-to-current conversion efficiencies (IPCE) of A: ZnO-nr photoelectrode before and after modification with FeS2 (a) and (b). B: ZnO-NP photoelectrode before and after modification with FeS_2 (a) and (b). Electrolyte was Na_2S 0.1M, Na_2SO_4 0.01M.

Although both have almost similar amount of FeS_2, this could only be understood in term unidirectional e-transport channels through nanorods (Fig. 7) with almost no hoping. Although, the photoresponse of ZnO-nr based pyrite solar cell is almost twice of that of ZnO-NP based pyrite cell, the performance of the cell is still low
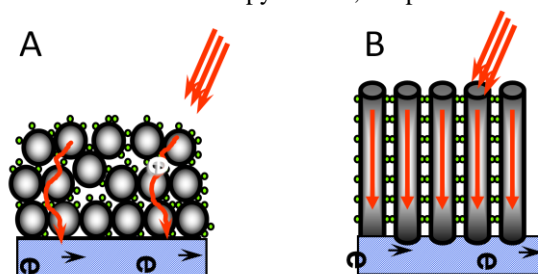

Fig. 7: Schemes (A) and (B) showing differences between electron transport in a mesorporous nanocrystalline ZnO film and nanorods ZnO film, respectively

compared to the best demonstrated pyrite photovoltaic device by MOCVD costly technique showing a modst 2.8% power conversion efficiency. Part of the reduced measured IPCE is due to the presence of large spaces seen in the ZnO-nr morphology which has helped aggregation of ultra fine FeS_2 particles inside the pores. This

may increase the chance of recombination of excited electrons in FeS_2 particles with the holes. This low performance was also partially explained by a high density of surface defects, but also the unusually low open circuit voltage of 200 mV, measured previously,[12, 23] suggests that phase purity may also play a alrge role. XRD spectrum (Fig. 5) in our case has showed the presence of multiphases of FeS_2 . Orthorombic marcasite FeS_2 and hexagonal troilite FeS are both common iron sulfure phases, but because they have much smaller band gaps (0.34 eV for marcasite and 0.04eV for troilite), even trace amounts would explain the low open circuit voltage about 200 mV [23] and low IPCE in our present work.

3.3 PIA spectroscopy
3.3.1 PIA Spectrum
Fig. 8 shows a typical PIA spectrum of FeS_2 modified ZnO-nr without electrolyte. The PIA spectrum clearly reflects the differential spectrum of FeS_2 upon formation injection of electrons to ZnO-nr, with a bleach of the main absorption around 470 nm. The remaining hole in FeS_2 absorbs light and because valence band electrons are missing, an apparent increase in bandgap is seen (bleach, Moss- Burstein shift). It has to be noted that no PIA spectrum for pyrite based ZnO-np photoelectrode has been recorded for comparison, and this is may be due to deep trapped electron sites and large number of boundaries in between ZnO nanoparticles which leads to a very low density of electrons which might leave and decay. For this case, only laser spectroscopy at high pulse intensity could detect that small intensity decay.
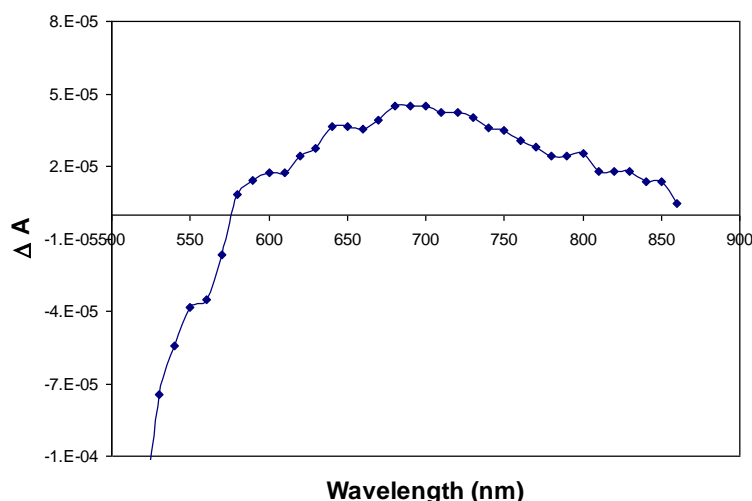

Fig. 8: Photoinduced absorption (PIA) spectum of quantum dots FeS2 Modified ZnO-nr electrode in air. The spectrum was recorded using blue light (460 nm) excitation (42 mW.cm-2) with a modulation frequency of 9 Hz.

3.3.2 PIA kinetics
Study of the kinetics in semiconductor sensitizing solar cells is not only feasible by laser flash photolysis, a costly technique, but also possible using time-resolved PIA measure-ments, a lower costly technique. Fig. 9 shows such a PIA transient growth recorded at 520 nm. (Pseudo-) first-order rate constant for bleach (growth at 520 nm) was about 0.15 ms, approximately, is due to hole-electron recombination which does not follow simple first-order kinetic but is characterized by a range of recombination times. This relatively fast decay proves at least a well pore filling of ZnO-nr film by ultra fine particles of pyrite.
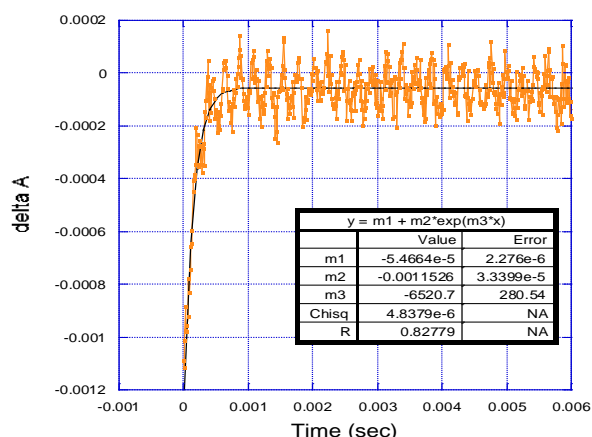
Fig. 9   PIA decay transient Absorption of quantum dots FeS_2 modified ZnO-nanorod electrode after excitation with blue light (11) mW/cm2) recorded at 520 nm, using a sampling rate of 10^3 s^{-1} and averaged 100 times.

IV.   CONCLUSION

The pyrite of iron disulfide (FeS_2) shows promise for solar energy conversion devices in photoelectrochemical solar cells. Photoinduced absorption spectroscopy where the excita-tion is provided by an on/off monochromatic light source can give direct information on electron-injection and hole-electron recombination rates using spectra of transient species and their kinetics can be explored using time-resolved techniques. PIA can monitor slow processes and is much lower costly compared to laser flash photolysis. ZnO-nr (1D network) based pyrite photoelectrode shows best photoresponse and e-transfer mechanistic than ZnO-np based pyrite solar cell. PIA demonstrates a good toold for studying any system based on ZnO nanorods. However the low performance of the cell in our case is explained by the presence of multiphase of FeS_2.

V.   AKNOWLEDGEMENT

REFERENCES

[1].   O'Regan, B.; Grätzel, M., A low-cost, high-efficiency solar cell based on dye-sensitized colloidal TiO_2 film, Nature 1991, 353, 737.

[2].   (a) I. Bedja, S. Hotchandani, P. V Kamat, and Photoelectrochemical Characterization of Thin SnO2 Nanocrystalline Semiconductor Films and Their Sensitization with Bis(2,2'-bipyridine)(2,2'-bipyridine-4,4'-dicarboxylic acid)ruthenium(II) Complex,J. Phys. Chem. **98**, 4133 (1994); (b) A. Hagfeldt, M. Gratzel,   (c) A. Hagfeldt, M. Gratzel, Molecular Photovoltaics, M. Acc. Chem. Res. **33**, 269 (2000)

[3].   **(a)** Bedja, I., Hotchandani, S. and Kamat,   Fluorescence and photoelectrochemical behavior of chlorophyll *a* adsorbed on a nanocrystalline SnO_2 film , J. Appl. Phys. 1996, 80, 8; (b) Guohua Wu,Ryuji Kaneko, Ashraful Islam, Idriss Bedja, Ravindra Kumar Gupta, Liyuan Han and Joe Otsuki , Effect of different auxiliary ligands and anchoring ligands on neutral thiocyanate-free ruthenium(II) dyes bearing tetrazole chromophores for dye-sensitized solar cells , Dyes and Pigments 140 (2017) 354-362

[4].   A. Yella, H.-W. Lee, H. N. Tsao, C. Yi, A. K. Chandiran, M. K. Nazeeruddin, E. W.-G. Diau, C.-Y. Yeh, S. M. Zakeeruddin, M. Grätzel, Porphyrin-sensitized solar cells with cobalt (II/III)-based redox electrolyte exceed 12 percent efficiency,Science, **334**, 629 (2011)

[5].   H. Choi;, J.G. Radish;, P.V. Kamat,   Sequentially Layered CdSe/CdS Nanowire Architecture for Improved Nanowire Solar Cell Performance, J. Phys. Chem. C, , **118**, 206 (2014)

[6].   Vogel, R., Hoyer, P. and Weller, H., Quantum-Sized PbS, CdS, Ag2S, Sb2S3, and Bi2S3 Particles as Sensitizers for Various Nanoporous Wide-Bandgap Semiconductors, J. Phys. Chem. 1994, 98, 3183.

[7].   Rabani, J.,   Sandwich colloids of zinc oxide and zinc sulfide in aqueous solutions, J. Phys. Chem. 1989, 93, 7707; S. Krishnamurthy, P. V. Kamat, CdSe–Graphene Oxide Light-Harvesting Assembly:

Size-Dependent Electron Transfer and Light Energy Conversion Aspects, ChemPhys Chem 15, 2129 (2014),

[8].   Bedja, I., Hotchandani, S. and Kamat, P. V., Photosensitization of composite metal oxide semiconductor films, J Berichte Der Bunsen-Gesselschaft-Physical Chemistry Chemical Physics, 1997, 101, 1651

[9].   Tributsch, H., Struct. Bonding, 1982, 49, 128

[10].   Tributsch, H, in: J.O. Bockris (Ed), Modern Aspects of Electrochemistry, 1986, 14, Pergamon Oxford, chap. 4

[11].   Bucher, E., Solar cell materials and their basic parameters, Appl. Phys. 1978, 17, 1

[12].   Ennaoui, S., Fiechter, H., Pettenkofer Ch., Alonso-Vantye, N., Bueker, K., Bronold, M., Hoepfner, Ch. and Tributsch, H., Iron disulfide for solar energy conversion, Solar Energy Materials and Solar Cells, 1993, 29, 289

[13].   Shen, Y., Deng, H., Fang, J. and Lu, Z., Colloids and Surfaces A: Physicochemical and Engineering Aspects 2000, 175, 135

[14].   Chatzitheodorou, G., Fiechter,S., Kunst, M. Luck, J. and Tributsch., H. , Low temperature chemical preparation of semiconducting transition metal chalcogenide films for energy conversion and storage, lubrication and surface protection, *Mat. Res. Bull.*, 1988, 23, 1261

[15].   Bauer, C.; Boschloo, G.; Mukhtar, E.; Hagfeldt, A., Electron Injection and Recombination in $Ru(dcbpy)_2(NCS)_2$ Sensitized Nanostructured ZnO, *J. Phys. Chem. B* **2001**, *105*, 5585.

[16].   Boschloo, G. and Hagfeldt, A., Photoinduced absorption spectroscopy as a tool in the study of dye-sensitized solar cells, Inorganica Chemica Acta 2008, 361, 729

[17].   Husk D. E. and Seehra, M. S., Solid State Commun., 1978, 27, 1142

[18].   Liu, C. Y. and Bard, J., Irradiation-induced absorption edge shifts in colloidal particles of iron (II) sulfide (pyrite), J. Phys. Chem. 1989, 93, 7047

[19].   Law M, Green L.E., Radenovic A, Kuykendall T, Liphard J. and Yang P.D., $ZnO−Al_2O_3$ and $ZnO−TiO_2$ Core−Shell Nanowire Dye-Sensitized Solar Cells, J. Phys. Chem. B 2006, 110, 22652;

[20].   Sheng Xu and Zhong Lin Wang, One-dimensional ZnO nanostructures: Solution growth and functional properties, Nano Res., DOI 10.1007/s12274-011-0160-7, June 2011

[21].   Huiling Zhao, Dong Chen, Bo Liu, Shuai Zhang, Mingdong Dong, Synthesis and Properties of One-dimensional ZnO Nanostructures and their Integration into Dye-sensitive Solar Cells, Nanoscience & Nanotechnology-Asia, Volume 2 , Issue 1 , 2012

[22].   Bedja I., "Photophysics and Photoelectrochemistry Studies on Nanocrystalline   Semiconductor Systems. Mechanistic studies of Photosensitization and Modulation of Electron Transfer Kinetics". Doctoral diss., University of Quebec at Trois-Rivieres, Quebec, Canada, 1996

[23].   Luther, G. Geochim. Cosmochim., Pyrite synthesis via polysulfide compounds, Acta, 55(10), (1991). 2839.